



VICTORIA UNIVERSITY
MELBOURNE AUSTRALIA

Protective efficacy of a plasmid DNA vaccine against transgene-specific tumors by Th1 cellular immune responses after intradermal injection

This is the Accepted version of the following publication

Son, Hye-Youn, Apostolopoulos, Vasso, Chung, June-Key, Kim, Chul-Woo and Park, Ji-Ung (2018) Protective efficacy of a plasmid DNA vaccine against transgene-specific tumors by Th1 cellular immune responses after intradermal injection. *Cellular Immunology*, 329. 17 - 26. ISSN 0008-8749

The publisher's official version can be found at
<https://www.sciencedirect.com/science/article/pii/S000887491830039X?via%3Dihub>
Note that access to this version may require subscription.

Downloaded from VU Research Repository <https://vuir.vu.edu.au/37261/>

1 **Protective efficacy of a plasmid DNA vaccine against transgene-specific**
2 **tumors by Th1 cellular immune responses after intradermal injection**

3
4 Hye-Youn Son, PhD¹, Vasso Apostolopoulos, PhD², June-Key Chung, MD, PhD³, Chul-Woo
5 Kim, MD, PhD^{4*}, Ji-Ung Park, MD^{1*}

6
7 ¹Department of Plastic and Reconstructive Surgery, Seoul National University Boramae
8 Medical Center, Seoul, Republic of Korea

9 ²Centre for Chronic Disease, College of Health and Biomedicine, Victoria University,
10 Melbourne, Victoria, Australia

11 ³Department of Nuclear Medicine, Cancer Research Institute, Seoul National University
12 College of Medicine, Seoul, Republic of Korea

13 ⁴Bioinfra Co. Ltd. 7th floor Cancer Research Institute, 49 Daehak-ro Yeongun-dong Jongro-gu,
14 Seoul, Republic of Korea

15
16 Corresponding authors:

17 Chul-Woo Kim. Bioinfra Co. Ltd. 7th floor Cancer Research Institute, 49 Daehak-ro Yeongun-
18 dong Jonro-gu, Seoul, Republic of Korea. Phone: +82-70-7006-2544; fax: +82-2-6499-7941;
19 e-mail: cwkim@snu.ac.kr

20
21 Ji-Ung Park. Department of Plastic and Reconstructive Surgery, Seoul National University
22 Boramae Medical Center, Seoul 07061, Korea. Phone: +82-2-2072-3086; fax: +82-2-831-2826;
23 e-mail: alfbskan@gmail.com

24
25 *These two authors contribute equally to this work as corresponding authors.

26 **Key words:** DNA vaccine, pCMV-LacZ, pcDNA-hNIS, IgG2a, tumor retardation

27

28 **Summary statement**

29 We used plasmid DNA like as LacZ DNA or NIS DNA which are internally translated in the
30 cells, which can be loaded on MHC I, not be secreted. We clarify reversion of immunity from
31 Th2 to Th1 when we repeated intradermal injection of plasmid DNA as a DNA vaccine.

32

33

34 **Running title:** Th1 response after intradermal DNA vaccination

35 **Abstract**

36 In evaluating the effectiveness of DNA vaccines, it is important to (1) monitor the movement
37 of cells transfected with the injected plasmid DNA; and (2) overcome immune deviation, which
38 causes a switch from helper T cell (Th)1 to Th2. Mouse CT26 cells were transfected with the
39 pcDNA-hNIS vector expressing human sodium/iodide symporter (hNIS) gene; the pCMV-
40 LacZ vector expressing β -galactosidase from the cytomegalovirus promoter was used for
41 imaging. Transgene expression was monitored by X-gal staining or γ -ray detection. Whole-
42 body images were obtained by nuclear scintigraphy following intraperitoneal injection of
43 radioactive technetium (^{99m}Tc). Migrating cells expressing hNIS or LacZ were monitored for 2
44 weeks. Reverse transcription PCR revealed that cells expressing the transgenes had moved out
45 of the injection site. hNIS-expressing cells were observed specifically in peripheral lymphoid
46 tissues, especially in draining lymph nodes and spleen. LacZ DNA was detected with a specific
47 antibody in immunized mice that exhibited Th2-type immunity. IgG2a type was predominant
48 in hNIS-immunized mice, as determined by enzyme-linked immunosorbent assay (ELISA).
49 Moreover, the vaccine caused increases in the IgG2a/IgG1 ratio, number of interferon (IFN)-
50 γ -secreting cells (by enzyme-linked immunospot assay), and IFN- γ level (by cytokine ELISA)
51 in the supernatant of immune cells. Tumor growth was retarded in mice that were immunized
52 with hNIS DNA followed by inoculation with CT26/NIS cells. The movement of mouse cells
53 transfected with plasmid DNA was restricted to immune organs. Transgene expression in these
54 cells was detected for at least 2 weeks post immunization. Repeated intradermal injection of
55 plasmid DNA caused a switch in the humoral immune response to the Th1 type.

56

57

58

59

60 **Introduction**

61 DNA vaccines can induce both cellular and humoral immunity and are considered as an
62 attractive immunization strategy to protect against infection, autoimmunity, and cancer
63 (Manthorpe et al., 1993; Ulmer et al., 1993; Wolff et al., 1990). The *LacZ* gene encoding β -
64 galactosidase (β -gal) has been used as a reporter for long-term imaging in gene therapy
65 experiments (Boland et al., 2000; Cho et al., 2002; Min et al., 2002). DNA vaccine injected
66 into a target site and internalized by antigen-presenting cells (APCs) without being degraded
67 can elicit a strong immune response in the host (Son et al., 2016a). The fate of injected DNA
68 vaccines can be monitored by examining their distribution or expression in the host (Donnelly,
69 Berry & Ulmer. 2003). For instance, DNA vaccines using *LacZ* injected via various routes has
70 been detected and shown to persist at the injection site as well as in other organs.
71 Biodistribution is primarily investigated by in situ hybridization, immunohistochemistry, and
72 reverse transcription (RT)-PCR, which require that experimental animals be sacrificed and their
73 organs isolated to confirm gene expression levels. In vivo imaging is required in order to
74 analyze gene expression following DNA vaccination in living animals.

75 Vaccination with the human sodium/iodide symporter (hNIS) gene combined with in
76 vivo monitoring has dual benefits—i.e., targeted immunotherapy against NIS-expressing
77 cancer cells and the ability to evaluate vaccine efficacy by scintigraphic imaging (*Son et al.*,
78 20167; *Jeon et al.*, 2007; *Jeon et al.*, 2008). ^{99m}Tc emits γ -rays; hNIS labeled
79 with ¹²⁴I, ¹²⁵I, ¹³¹I, or ^{99m}Tc has allowed the visualization of various biochemical processes in
80 the tissues of living subjects (Son et al., 2016a).

81 We used *LacZ* and NIS as reporter genes to monitor immune responses following DNA
82 immunization. Cytoplasmic *LacZ* and transmembrane NIS proteins are translated and retained
83 in cells without being secreted. Moreover, they can be loaded onto major histocompatibility
84 complex class (MHC-)I after translation and onto MHC-II after engulfment by APCs, thereby

85 stimulating helper T cell (Th)1 and Th2 immune responses, and finally avoiding immune
86 deviation (Son et al., 2016b).

87 Modulating the tumor microenvironment is a critical aspect of cancer immunotherapy
88 (Kuol et al., 2017). hNIS has been used to overcome the challenges posed by the complexity
89 of the tumor microenvironment. Expression of NIS—a specialized active iodide transporter
90 (Chungl, 2002; De La Vieja et al., 2000)—results in the accumulation of therapeutic
91 radionucleotides in cancer cells (Chen et al., 2006; Mandell, Mandell & Link 1999). However,
92 the efficacy of targeting cancer cells by hNIS radioiodine gene therapy and thereby modifying
93 antitumor immunity has not been systematically investigated in here.

94 Normally, intradermal (i.d.) injection (Yu et al., 1999) induces antigen-specific Th2
95 immune responses. However, in the present study, we performed repeated i.d. injections
96 (Michael et al. 1999; Shedlock & Weiner, 2000) of a naked DNA vaccine consisting of plasmid
97 DNA encoding *hNIS* and the *lacZ* gene as a marker to induce Th1 response. We monitored the
98 distribution and persistence of gene expression and evaluated the capacity for inducing specific
99 Th1 immune responses in the context of a Th2-dominant immune profile. We found that an
100 anti-LacZ humoral and anti-hNIS Th1 immune responses were induced by repeated i.d.
101 immunizations and the use of non-secreted proteins encoding genes that solve immune
102 deviation (Son et al., 2016b).

103

104

105 **Materials and Methods**

106 *Plasmid DNA*

107 The hNIS-expressing vector pcDNA3.1-FL-hNIS vector (pcDNA-hNIS) expressing hNIS
108 under the control of the cytomegalovirus (CMV) promoter and the neomycin resistance cassette
109 from the simian virus 40 promoter was provided by Dr. S. Jhiang (Ohio State University,

110 Columbus, OH, USA). The pCMV β vector expressing β -gal was purchased from Clontech
111 (Mountain View, CA, USA). Plasmids were amplified in *Escherichia coli* DH5 α cells and
112 purified using endotoxin-free Giga Prep columns (Qiagen, Valencia, CA, USA).

113 *Detection of enhanced green fluorescent protein plasmid (pEGFP) in CT26 cells*

114 The day before transfection, CT26 cells grown in a 75-cm² flask were trypsinized, and 10% of
115 each cell line was mixed in 18 ml of Medium 199 (Hyclone, Logan, UT, USA) supplemented
116 with 10% fetal bovine serum (FBS); 3 ml of this cell suspension was seeded into one well of a
117 6-well plate using Transfast reagent (Promega, Madison, WI, USA) according to the
118 manufacturer's instructions. Briefly, 2 ml of the reagent and 1 mg of pEGFP plasmid were
119 mixed and incubated at room temperature for 15 min. The mixture was added to the cells and
120 6 h later, the DNA-transfection mixture was replaced with Medium 199. After 48 h,
121 fluorescence was detected by using flow cytometry on a FACSAria instrument (BD
122 Biosciences, San Jose, CA, USA).

123

124 *β -gal staining of transfected CT26 cells*

125 The plasmid encoding *lacZ* was transfected as described above. Cells were then washed three
126 times for 5 min at room temperature and then fixed in a solution of 2% formaldehyde and 0.2%
127 glutaraldehyde in phosphate-buffered saline (PBS; pH 7.6–7.8) for 5 min at room temperature.
128 After rinsing with PBS, substrate solution (1 mg/ml X-gal substrate; Sigma-Aldrich,
129 Deisenhofen, Germany) was added, followed by incubation at 37°C for 6 h. Transfection
130 efficiency was visually confirmed.

131

132 *Detection of hNIS expression in CT26 cells*

133 The plasmid encoding NIS DNA was transfected as described above. The ability of transfected
134 cells to concentrate ^{99m}Tc or ¹³¹I was determined as previously described [14]. Briefly, CT26

135 cells (5×10^4) were seeded in 24-well plates and cultured in Dulbecco's Modified Eagle's
136 Medium (DMEM) containing 10% FBS for 24 h. ^{125}I uptake was determined by incubating
137 cells with 500 μl of Hank's balanced salt solution (bHBSS; Gibco, Grand Island, NY, USA)
138 containing 3.7 kBq of carrier-free ^{125}I and 10 μM sodium iodide (NaI) at 37°C for 30 min to
139 obtain a specific activity of 740 MBq/mmol (20 mCi/mmol). The cells were quickly washed
140 twice with bHBSS and detached using 500 μl trypsin. Radioactivity was measured using a
141 gamma counter (CobraII Packard; PerkinElmer, Waltham, MA, USA).

142

143 *Immunization*

144 Specific pathogen-free female BALB/c mice (6 weeks old) were obtained from SLC Japan
145 (Hamamatsu, Japan) and were handled according to the guidelines issued by the Seoul National
146 University Animal Research Committee. For in vivo tracking of plasmid vectors, 100 μg of
147 pCMV-LacZ or pcDNA-hNIS resuspended in 50 μl endotoxin-free Tris-
148 ethylenediaminetetraacetic acid buffer (Qiagen) were administered by i.d. injection into the
149 thigh of mice using a 30-G insulin syringe (BD Biosciences, Franklin Lakes, NJ, USA). To
150 identify tumor-protective or antigen-specific cellular immune responses, mice were immunized
151 three times at 2-week intervals in the hind leg with *hNIS* DNA or in the dorsal skin with *lacZ*
152 DNA. Mice were anesthetized by intraperitoneal injection of 0.3 ml of a 1:1:9 solution of
153 rompun, (Parke-Davis, Detroit, MI, USA), ketamine (Bayer, Leverkusen, Germany), and saline
154 (RKS solution).

155

156 *PCR detection of lacZ and hNIS plasmid DNA*

157 PCR primers were designed to amplify the *lacZ* gene in dorsal skin and *hNIS* gene in various
158 organs, including the draining lymph nodes (dLNs), non-dLNs, spleen, muscle, liver, and heart.

159 The forward and reverse sequences were as follows: *lacZ*, 5'-

160 TTCACTGGCCGTCGTTTTACAACGTCGTGA-3' and 5'-
161 ATGTGAGCGAGTAACAACCCGTCGGATTCT-3'; and *hNIS*, 5'-
162 AGATGAGCTGACACGGAACAG-3' and 5'-CTGGGGAAAAGTGGGAAAAGAG-3'.

163 Expression levels were normalized to that of β -actin (5'-CTGTGCTATCCCTGTACGCC-3'
164 and 5'-ATGTGACAGCTCCCCACACA-3'). The 50- μ l reaction contained 5 μ l PCR buffer, 50
165 nM each dNTP, 5 nM forward and reverse primers, and 1 U Taq DNA polymerase. The PCR
166 conditions were as follows: 94°C for 5 min; 35 cycles of 94°C for 45 s, 63°C for 45 s, and 72°C
167 for 45 s; and 72°C for 7 min. PCR products were resolved on a 2% agarose gel and visualized
168 under ultraviolet light. PCR conditions for transgene amplification were as follows: 34 cycles
169 of 94°C for 60 s, 55°C for 60 s, and 72°C for 60 s.

170

171 *hNIS* reverse transcription (RT)-PCR

172 Organs were removed from immunized mice and lysed using a homogenizer. Total RNA was
173 extracted from lysates in the presence of RNase inhibitors using TRIzol reagent (Molecular
174 Research Center, Cincinnati, OH, USA). Isolated RNA was dissolved in diethyl pyrocarbonate-
175 treated water (Sigma-Aldrich, St. Louis, MO, USA) and used to generate cDNA using a 15-
176 mer poly dT oligonucleotide (Invitrogen, Carlsbad, CA, USA) and Superscript reverse
177 transcriptase (Gibco) with incubation at 37°C for 1 h according to the manufacturer's protocol.
178 Expression of the *hNIS* gene was detected in dLNs, non-dLNs, and spleen by RT-PCR using
179 the primers: 5'-GGCTCCTCGGTGACTCTAGGATGC-3' (forward) and 5'-
180 CATGAATTCTGGGCTCAATTTTCTTGTC-3' (reverse). To confirm DNA integrity, the
181 mouse β -actin gene (codons 135–223) was amplified with the primers 5'-
182 GGCTCCTCGGTGACTCTAGGATGC-3' (forward) and 5'-
183 CATGAATTCTGGGCTCAATTTTCTTGTC-3' (reverse) under the following conditions: 34
184 cycles of 94°C at 60 s, 55°C at 60 s, and 72°C at 60 s.

185

186 *Whole-body imaging and nuclear scintigraphy of hNIS DNA-immunized mice*

187 At designated times (2, 16, and 24 h and 2, 3, and 11 days) following injection of pcDNA-
188 hNIS, mice were administered 300 μ Ci of ^{99m}Tc (11.1 MBq) by intraperitoneal injection and
189 anesthetized with 0.3 ml of RKS solution; 30 min later, mice were placed in a prostrate position
190 and scanned with a gamma camera (ON 410; Ohio Nuclear, Solon, OH, USA) equipped with
191 a pinhole collimator. Relative radioactivity was assessed in the entire body over a period of 5
192 min, and dynamic frames were obtained; 1 h later, LNs, spleen, liver, and skin near the injection
193 site were removed from each mouse and weighed to determine the organ distribution patterns
194 of injected DNA; blood samples were also collected. Tissues were stored at -70°C for 16 h,
195 after which ^{99m}Tc uptake was measured using a gamma counter.

196

197 *Antibody measurements by enzyme-linked immunosorbent assay (ELISA)*

198 Antibody titers in sera obtained from mice at the end of the experiment were determined by
199 ELISA. Briefly, 96-well microtiter plates were coated overnight with 1 mg β -galactosidase (5
200 mg/ml) in 0.1 M carbonate buffer (pH 9.5) for detection of anti- β -gal antibodies. To determine
201 anti-NIS antibody titer, 96-well microtiter plates were coated with 1×10^4 irradiated CT26 or
202 CT26/NIS cells in 0.01 M PBS (pH 7.5). After washing with wash buffer (PBS with 0.05%
203 Tween-20 [pH 7.4]), the plates were blocked overnight with assay diluent (BD Pharmingen,
204 San Diego, CA, USA). After washing with wash buffer, eight consecutive 1:3 dilutions of
205 serum sample in assay diluent initially diluted 1:20, 1:40, and 1:100 (for detection of anti- β -
206 gal antibodies) were added to the wells. After 2 h of incubation at room temperature, the plates
207 were washed with wash buffer and incubated for 1 h at room temperature with horseradish
208 peroxidase (HRP)-conjugated goat anti-mouse immunoglobulin (Ig; Southern Biotechnology
209 Associated, Birmingham, AL, USA). HRP-conjugated goat anti-mouse IgG1 or IgG2a

210 (Southern Biotechnology Associated) were used to determine the isotype of the antibodies.
211 After washing, 100 µl of substrate solution (tetramethylbenzidine and hydrogen peroxide; BD
212 Pharmingen) were added, and the plate was incubated in the dark for 30 min at room
213 temperature. The reaction was terminated by adding 1 M H₂SO₄ and absorbance was measured
214 at 450 nm on an ELISA plate reader. To calculate anti-NIS and total antibodies titers, purified
215 mouse IgG2a or IgG1 monoclonal antibodies were included in the plates.

216

217 *Enzyme-linked immunospot (ELISpot) assay*

218 Th1 interferon (IFN)-γ or Th2 interleukin (IL)-4 secretion by stimulated T cells were evaluated
219 with commercially available ELISpot assay kits (Diaclone, Besançon, France) according to the
220 manufacturer's protocol. Briefly, PVDF polyvinylidene difluoride 96-well plates were
221 incubated overnight at 4°C with an anti-mouse IFN-γ or -IL-4 (capture) antibody. The
222 following day, freshly isolated NIS-immunized LN cells (5×10^5 responder cells/well) were
223 washed and resuspended in Roswell Park Memorial Institute (RPMI) 1640 medium containing
224 10% fetal calf serum and then incubated in anti-INF-γ or -IL-4 antibody-pre-coated 96-well
225 plates at 37°C for 20 h. The cells were removed, and biotinylated anti-mouse IFN-γ or IL-4
226 (detection) antibodies were added followed by streptavidin-conjugated alkaline phosphatase,
227 which converted the substrate 5-bromo-4-chloro-3-indolyl phosphate/nitro blue tetrazolium to
228 a blue dye. Spots were counted using the Bioreader system (BIO-SYS GmbH, Karben,
229 Germany).

230

231 *Cytokine ELISA*

232 LNs were removed and single-cell suspensions were obtained by gentle pipetting.
233 Lymphocytes were washed and resuspended in RPMI 1640 medium supplemented with 10%
234 heat-inactivated FBS, 2 mM L-glutamine, 200 mg/ml streptomycin, 200 U/ml penicillin, and

235 0.1% 2-mercaptoethanol. Cells were seeded in 24-well tissue culture plates at a final
236 concentration of 2×10^6 /ml in enriched RPMI 1640 medium, and stimulated by co-culturing
237 with irradiated CT26 or CT26/NIS cells for 72 h at 37°C in an atmosphere of 5% CO₂. IL-4
238 and INF- γ levels in culture supernatants of LN cells stimulated with irradiated CT26 or
239 CT26/NIS cells were measured using OptEIA mouse IFN- γ or IL-4 ELISA kits (BD
240 Pharmingen) according to the manufacturer's instructions.

241

242 *Tumor challenge*

243 At 2 weeks after the final hNIS DNA injection, mice were challenged by subcutaneous injection
244 into the fore leg of 5×10^5 (left) or 1×10^5 (right) CT26/NIS cells resuspended in 100 μ l of
245 10% FBS in DMEM. Tumor dimensions were measured twice a week, and tumor volume was
246 calculated as horizontal length (mm) \times vertical length (mm) \times depth (mm) = volume (in mm³).

247

248 *In vivo tumor imaging*

249 At indicated times after injection of pcDNA NIS into CT26/NIS tumors, 37 MBq of ^{99m}Tc was
250 injected into the tail of mice and static SPECT images were acquired after 10 min using a
251 gamma camera (GE Healthcare, Waukesha, WI, USA) with a low-energy, high-resolution
252 collimator.

253

254 *Biodistribution study*

255 Mice were sacrificed at the end of the single-photon emission computed tomography (SPECT)
256 scan (90-min time point). Blood, heart, liver, spleen, lung, kidneys, thyroid, stomach, intestine,
257 muscle, bone, and tumor were harvested and weighed. Radioactivity was measured with a
258 gamma counter and the corresponding counts per million/mg tissue was calculated.

259

260

261 **Results**

262 **Efficiency of plasmid DNA expression**

263 We evaluated the transfection efficiency of each plasmid into CT26 murine colon cancer cells
264 (H-2d; syngeneic in BALB/c mouse strain). EGFP expression was detected by flow cytometry
265 (Fig. 1A). *LacZ* in CT26 cells was visible as a green color (Fig. 1B). The transfection efficiency
266 was confirmed with pcDNA3.1-hNIS by detecting ^{99m}Tc with a gamma counter (Fig. 1C).
267 These results demonstrate that the plasmid vectors are able to transfect cells.

268

269 **β-gal is expressed in mouse tissues following pCMV-LacZ inoculation**

270 X-gal is an organic compound composed of galactose linked to indole that is commonly used
271 to test for the presence of β-gal according to a color change to blue/green. We monitored β-gal
272 expression in mouse skin following i.d. injection of pCMV-LacZ by X-gal staining. Although
273 there was no spread of the blue dye beyond the injection site (Fig. 2A, left panel), the green
274 color corresponding to X-gal was detected far away from the injection site from 2 h to 30 days
275 post-injection (Fig. 2A, right panel), suggesting that the plasmid encoding the *lacZ* gene was
276 taken up by resident cells (most likely keratinocytes or APCs) that then migrated out of the
277 injection site. We next evaluated the levels of pCMV-LacZ DNA injected into the dorsal skin,
278 which was divided into three sites (Fig. 2B, upper): sections 1, 2, and 3 represent the upper,
279 middle, and lower sites of injection, respectively. The PCR analysis revealed that DNA had
280 moved from the injection site throughout the body up until 10 days after injection (Fig. 2B,
281 lower). *LacZ* DNA was still detected at the injection site at 15 and 30 days.

282

283 **hNIS gene is expressed in mouse tissues following DNA inoculation**

284 Our data suggested that cells transfected with plasmid DNA and injected into mice could

285 migrate away from the injection site. We therefore evaluated the expression of *hNIS* DNA in
286 various immune tissues of mice (LN and spleen) and other organs (muscle, heart, and liver)
287 following i.d. injection. *hNIS* DNA was expressed in lymph nodes as early as 2 h post-injection
288 and in the spleen after 3 days, with expression persisting up to day 18; at 2 h, *hNIS* DNA was
289 detected in muscle tissues at the injection site (Fig. 3A). An RT-PCR analysis showed that *hNIS*
290 was expressed as early as 2 h post-injection in the LN and after 1 day in the spleen, with
291 expression persisting up to 18 days; in contrast, mock transfectants showed no *hNIS* expression
292 (Fig. 3B).

293 To monitor NIS expression, we dissected the organs and detected γ -rays with a gamma
294 counter. At 2 h post-injection, γ -ray levels were highest at the injection site (skin) relative to
295 the mock-injected group (Fig. 4A). Up to 11 days after DNA injection, ^{99m}Tc uptake was highest
296 in lingual LNs (dLN), followed by the LN (non-dLN) and spleen (Fig. 4B, C). To quantify the
297 level of radioactivity in vivo, regions of interest in the scintigraphic images were analyzed at
298 various time points (2, 8, 16, and 24 h and 11 days) after immunization. Whole-body relative
299 radioactivity levels adjacent to the injection site were higher in mice immunized with *hNIS*
300 plasmid as compared to mock-injected control mice (Fig. 4D). As expected, *hNIS* gene
301 expression was detected in the LN and spleen for up to 11 days.

302

303 **Humoral and cellular responses induced by repeated i.d. injections of *lacZ* and *hNIS* DNA**

304 Determining the mechanism by which DNA vaccines stimulate the immune response is critical
305 for identifying the type of immune response that is induced [19, 20]. While i.d. delivery will
306 firstly elicit the humoral response with the release of IgA and IgG1, the intramuscular route has
307 been shown to prime cellular responses by activation of cytotoxic T lymphocytes (CTLs) and
308 production of IgG2a. We therefore evaluated antibody responses against *lacZ*. Anti β -gal
309 antibodies were generated at 10 days, with the levels reaching a peak at 15 days post-

310 immunization (Fig. 5A). The antibody subclass was assessed by ELISA by coating the wells
311 with NIS-expressing CT26 cells and adding serum from mice immunized with pcDNA or hNIS
312 DNA. The results show that the anti-NIS antibodies generated were of the IgG2a (Th1) isotype
313 (Fig. 5B).

314

315 **hNIS DNA vaccination induces a strong Th1 cytokine profile**

316 The ELISpot assay was used to evaluate the secretion of IFN- γ and IL-4 by cells isolated from
317 dLNs, non-dLNs, mesenteric (M) LNs and spleen after NIS DNA immunization. To assess
318 hNIS-specific T cell responses, splenocytes and LN cells were isolated 10 days after the final
319 injection. IFN- γ was secreted at a high level by cells from the dLN and to a lesser extent by
320 MLN and non-dLN cells; the spleen also showed a specific anti-NIS IFN- γ response (Fig. 6A).
321 IL-4 was not detected. These data were confirmed by in vitro stimulation of spleen, dLN, and
322 non-dLN cells with irradiated CT26/NIS cells and measurement of cytokine secretion by
323 ELISA. Similar to the results of the ELISpot assay, high levels of IFN- γ were secreted by cells
324 of dLNs relative to non-dLN and spleen, with no IL-4 secretion (Fig. 6B).

325

326 **Protective tumor immunity induced by DNA immunization**

327 We investigated whether immunization of mice with hNIS DNA conferred protection against
328 tumors expressing NIS. Mice were subcutaneously inoculated with CT26/NIS tumor cells 2
329 weeks after the final *hNIS* DNA injection (Fig. 7A). Mice immunized with *hNIS* DNA showed
330 significant retardation of tumor growth relative to those injected with pcDNA3 (Fig. 7B).
331 Evaluation of tumor mass by ^{99m}Tc uptake measurements for up to 33 days confirmed these
332 observations.

333

334

335 **Discussion**

336 Plasmid DNA injection can lead to transgene expression in vivo (Wolff et al., 1990; Chen et
337 al., 2013; Han et al., 2015). However, immune responses induced by DNA vaccines have not
338 been extensively, although they are thought to be similar to the viral infection process.
339 Immediately after injection, plasmid DNA enters cells—mainly keratinocytes and APCs
340 (Tonheim, Bogwald & Dalmo, 2008)—and is transported to the nucleus. The transgene is
341 transcribed and then translated into a protein that is presented by MHC-I or -II to the host
342 immune system. The protein may then be engulfed and degraded, while transgene peptide-
343 loaded APCs can migrate to dLNs to activate naïve T cells (Son et al., 2016).

344 In this study, we found that the transgene spread far from the site of injection following
345 in vivo inoculation and was detected up to 30 days post-inoculation. The transgene-expressing
346 cells migrated primarily into immune organs such as dLNs, suggesting that the cells are APCs
347 that home to immune organs to activate an inflammatory signal, or else keratinocytes that are
348 targets for the immune response. In the LNs, Th cells activated by transgene-expressing APCs
349 secrete cytokines that can activate B cells to induce an anti- β -gal humoral response and the
350 production of IgG2a anti-NIS antibodies by isotype switching (Boland et al., 2000). Antigen-
351 binding B cells are trapped in the T cell-rich zone of dLNs and are activated by encounters with
352 activated Th cells. Antibody isotype switching is stimulated by multiple cytokines. IL-4
353 induces a switch to IgG1 and IgE, whereas transforming growth factor (TGF)- β causes a switch
354 to IgG2b and IgA. Th2 cells secrete IL-4 and -5 and TGF- β , which induce IgA. Although Th1
355 cells are poor initiators of antibody responses, they release IFN- γ for antibody isotype
356 switching to IgG2a and IgG3 (Janeway et al., 2001). In our study, we confirmed IgG2a
357 switching after DNA vaccination, which corresponded to an increase in IFN- γ levels. It is
358 possible that antibody isotype switching ultimately leads to tumor killing by the Th1 response,
359 which activates cytotoxic T cells. Soluble or secreted vaccine antigens may be phagocytosed

360 by APCs immediately following DNA vaccination and enter the MHC class II exogenous
361 pathway. We therefore used a cellular (LacZ) or transmembrane (NIS) protein to exclude direct
362 APC uptake immediately after translation that could deviate into Th2-type immune responses.
363 We also administered two booster injections to re-activate cellular immunity. The immune
364 response to the first immunization was predominantly humoral; however, memory T cells were
365 subsequently recruited to the injection site, which stimulated a Th1-type immune response (Son
366 et al., 2016b). Repeated immunization (boosting) involves dendritic cells (DCs), but it is
367 unclear how frequently booster injections should be administered. In fact, a homologous prime-
368 boost strategy may not be ideal, as antigen-bearing DCs were shown to be eliminated by
369 effector and memory CTLs in vaccinated mice (Yang et al., 2006).

370 CD8⁺ T cells can lyse cells presenting transgenic peptide on MHC-I molecules,
371 resulting in increased antigen release. Furthermore, CD4⁺ T cells (Th2 response) can activate
372 immature DCs that home to LNs and stimulate B and T cells (Reyes-Sandoval and Ertl, 2001),
373 thereby repeating the cycle of activation. Thus, both humoral and cellular immunity are primed
374 for the next challenge although CD8⁺ T cells must be induced to lyse tumor cells. It was
375 previously shown that i.d. injection can result in a Th2-type profile (Shedlock and Weiner,
376 2000), but in this study we observed that humoral immunity could be induced to switch to Th1-
377 type immunity (IgG2a). Furthermore, IFN- γ was significantly induced in the transgene-
378 immunized group relative to controls, which protected the mice from tumor challenge. The
379 presumed mechanism is shown in Figure 8.

380 Although DNA vaccines can induce cellular responses, the injection route is an
381 important determinant of the type of response. A Th2 response is typically induced by i.d.
382 injection of DNA (*Shedlock & Weiner, 2000*), posing a challenge for the widespread use of
383 DNA vaccines. In this study, we solved this problem by inhibiting the Th2 response through
384 IgG1 to IgG2a switching. We selected an intracellular antigen that can be loaded onto MHC-I

385 to activate the Th1 response and administered repeated, which could induce memory T cells
386 and can easily stimulate a Th1-type response. Additional studies are needed to determine
387 whether memory T cells are upregulated after repeated i.d. injection of plasmid DNA.

388

389

390 **Funding**

391 This work was supported by the SNUH Research Fund (grant no. 04-2016-0670). The funders
392 had no role in study design, data collection and analysis, decision to publish, or preparation of
393 the manuscript.

394

395

396 **Competing Interests**

397 The authors declare there are no competing interests.

398

399

400 **References**

401 **Boland, A., Ricard, M., Opolon, P., Bidart, J. M., Yeh, P., Filetti, S., Schlumberger, M.,**
402 **and Perricaudet, M.** (2000). Adenovirus-mediated transfer of the thyroid sodium/iodide
403 symporter gene into tumors for a targeted radiotherapy. *Cancer Research* **60**:3484–92.

404 **Chen, L., Altmann, A., Mier, W., Eskerski, H., Leotta, K., Guo, L., Zhu, R., and**
405 **Haberkorn, U.** (2006). Radioiodine therapy of hepatoma using targeted transfer of the human
406 sodium/iodide symporter gene. *The Journal of Nuclear Medicine* **47**:854–62.

407 **Chen, Y. Z., Ruan, G. X., Yao, X. L., Li, L. M., Hu, Y., Tabata, Y., and Gao, J. Q.** (2013).
408 Co-transfection gene delivery of dendritic cells induced effective lymph node targeting and
409 anti-tumor vaccination. *Pharmaceutical Research* **6**:1502–12.

410 **Cho, J. Y., Shen, D. H., Yang, W., Williams, B., Buckwalter, T. L., La Perle, K. M., Hinkle,**
411 **G., Pozderac, R., Kloos, R., Nagaraja, H. N., Barth, R. F., and Jhiang, S. M.** (2002). In
412 vivo imaging and radioiodine therapy following sodium iodide symporter gene transfer in
413 animal model of intracerebral gliomas. *Gene Therapy* **9**:1139–45.

414 **Chung JK.** (2002). Sodium/iodide symporter: its role in nuclear medicine. *The Journal of*
415 *Nuclear Medicine* **43**:1188–200.

416 **De La Vieja, A., Dohan, O., Levy, O., and Carrasco, N.** (2000). Molecular analysis of the
417 sodium/iodide symporter: impact on thyroid and extrathyroid pathophysiology. *Physiological*
418 *Review* **80**:1083–105

419 **Donnelly, J., Berry, K., and Ulmer, J. B.** (2003). Technical and regulatory hurdles for DNA
420 vaccines. *International Journal for Parasitology* **33**:457–67

421 **Han, Y., Li, X., Zhou, Q., Jie, H., Lao, X., Han, J., He, J., Liu, X., Gu, D., He, Y., and Sun,**
422 **E.** (2015). FTY720 abrogates collagen-induced arthritis by hindering dendritic cell migration
423 to local lymph nodes. *Journal of Immunology* **195**:4126–35.

424 **Janeway, C. A., Travers, P Jr., Walport, M., and Shlomchik, M. J.** (2001). Immunobiology:
425 The Immune System in Health and Disease. 5th edition. *New York: Garland Science*

426 **Jeon, Y. H., Choi, Y., Kim, H. J., Kim, C. W., Jeong, J. M., Lee, D. S., and Chung, J. K.**
427 (2007). Human sodium/iodide symporter gene adjunctive radiotherapy to enhance the
428 preventive effect of hMUC1 DNA vaccine. *International Journal of Cancer* **121**:1593–9.

429 **Jeon, Y. H., Choi, Y., Yoon, S. O., Kim, C. W., and Chung, J. K.** (2008). Synergistic
430 tumoricidal effect of combined hMUC1 vaccination and hNIS radioiodine gene therapy.
431 *Molecular Cancer Therapeutics* **7**:2252–60.

432 **Kuo, I N., Stojanovska, L., Nurgali, K., and Apostolopoulos, V.** (2017). The mechanisms
433 tumor cells utilise to evade the hosts immune system. *Maturitas* **105**:16-22

434 **Mandell, R. B., Mandell, L. Z., and Link, C. J Jr.** (1999). Radioisotope concentrator gene

435 therapy using the sodium/iodide symporter gene. *Cancer Research* **59**:661–8.

436 **Manthorpe, M. I., Cornefert-Jensen, F., Hartikka, J., Felgner, J., Rundell, A., Margalith,**
437 **M., and Dwarki, V.** (1993). Gene therapy by intramuscular injection of plasmid DNA: studies
438 on firefly luciferase gene expression in mice. *Human Gene Therapy* **4**:419–31

439 **Michael, J., McCluskie, Cynthia, L., Brazolot M., Robert A. Gramzinski, Harriet L.,**
440 **Robinson, J. C., Santoro, J. T., Fuller, G. W., Joel, R., Haynes, R. H., Purcell, Heather, L.,**
441 **and Davis, L.** (1999). Molecular Medicine Route and Method of Delivery of DNA Vaccine
442 Influence Immune Responses in Mice and Non-Human Primates. *Molecular Medicine* **5**: 287-
443 300

444 **Min, J. J., Chung, J. K., Lee, Y. J., Shin, J. H., Yeo, J. S., Jeong, J. M., Lee, D. S., Bom, H.**
445 **S., and Lee, M. C.** (2002). In vitro and in vivo characteristics of a human colon cancer cell
446 line, SNU-C5N, expressing sodium-iodide symporter. *Nuclear Medicine Biology* **29**:537–45.

447 **Reyes-Sandoval, A., and Ertl, H. C.** (2001). DNA vaccines. *Current Molecular Medicine*
448 **1**:217–43

449 **Shedlock, D. J., and Weiner, D. B.** (2000). DNA vaccination: antigen presentation and the
450 induction of immunity. *Journal of Leukocyte Biology* **68**:793–806.

451 **Son, H. Y., Jeon, Y. H., Jung, J. K., and Kim, C. W.** (2016a) In vivo monitoring of transfected
452 DNA, gene expression kinetics, and cellular immune responses in mice immunized with human
453 NIS gene-expressing plasmid. *International Journal of Immunopathology and Pharmacology*
454 **29**:612-25

455 **Son, H. Y., Apostolopoulos, V., and Kim, C. W.** (2016b) T/Tn immunotherapy avoiding
456 immune deviation. *International Journal of Immunopathology and Pharmacology* **29**:812-817

457 **Tonheim, T. C., Bogwald, J., and Dalmo, R. A.** (2008). What happens to the DNA vaccine
458 in fish? A review of current knowledge. *Fish and Shellfish Immunology* **25**:1–18

459 **Ulmer, J. B., Donnelly, J. J., Parker, S. E., Rhodes G. H., Felgner, P. L., Dwarki, V. J.,**

460 **Gromkowski, S. H., Deck, R. R., and DeWitt, C. M.** (1993). A Friedman Heterologous
461 protection against influenza by injection of DNA encoding a viral protein. *Science* **259**:1745–
462 9

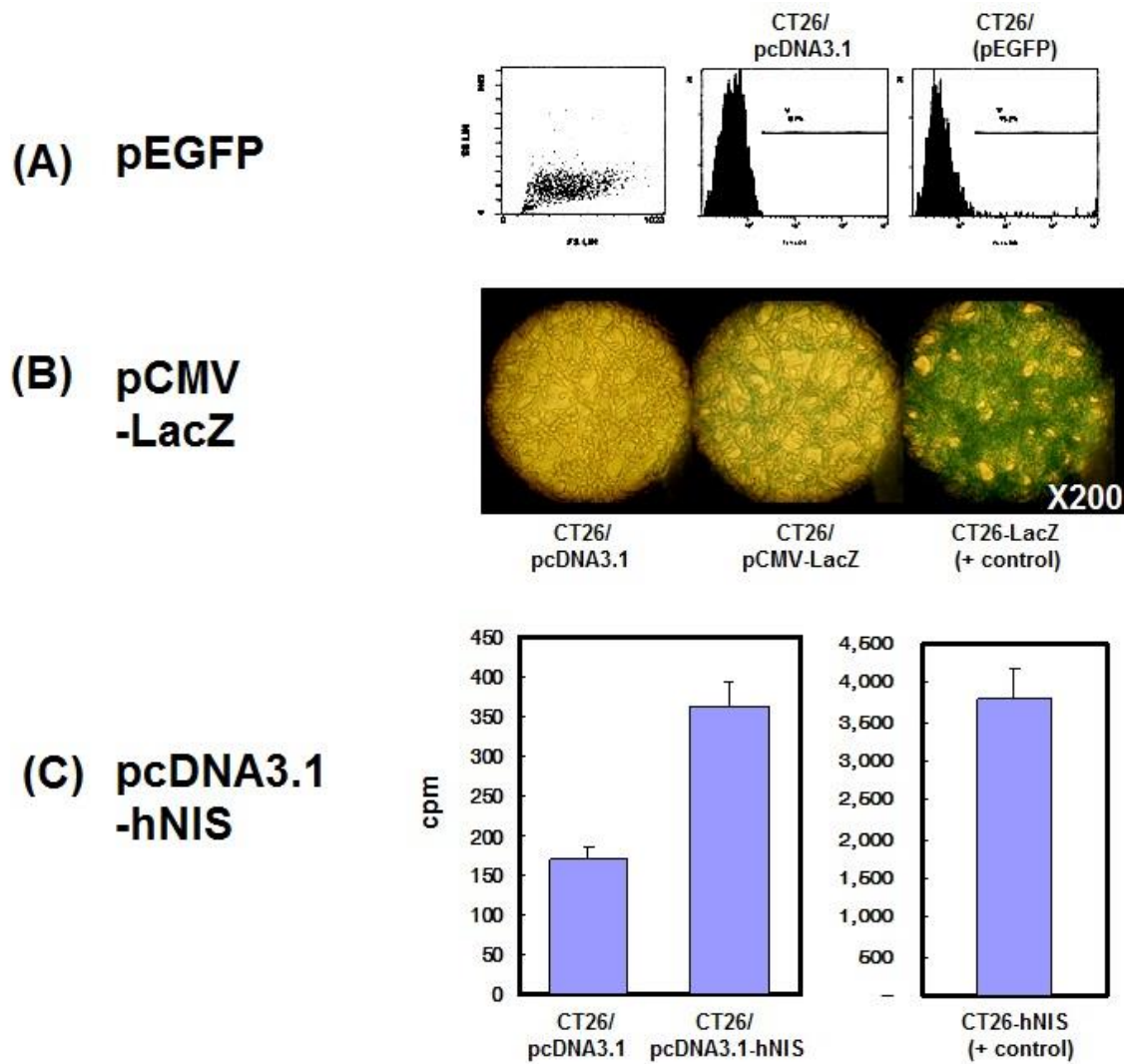
463 **Wolff, J. A., Malone, R. W., Williams, P., Chong, W., Acsadi, Q., Jani, A., and Felgner, P.**
464 **L.** (1990). Direct gene transfer into mouse muscle in vivo. *Science* **247**:1465–8.

465 **Yang, J., Huck, S. P., McHugh, R. S., Hermans, I. F., and Ronchese, F.** (2006). Perforin-
466 dependent elimination of dendritic cells regulates the expansion of antigen-specific CD8+ T
467 cells in vivo. *Proceedings of the National Academy of Sciences of the United States of America*
468 **103**:147-52.

469 **Yu, W. H., Kashani-Sabet, M., Liggitt, D., Moore, D., Heath, T. D., and Debs, R. J.** (1999).
470 Topical gene delivery to murine skin *Journal of Investigative Dermatology* **112**:370-5.
471
472
473

474

475 **Figure legends**



476

477 **Figure 1. In vitro expression of various plasmid DNAs in CT26 cells.** (A) Transfection

478 efficiency and eGFP expression were evaluated by flow cytometry 48 h after transfection. (B)

479 X-gal staining was performed following pCMV-LacZ transfection. (C) ^{99m}Tc uptake was

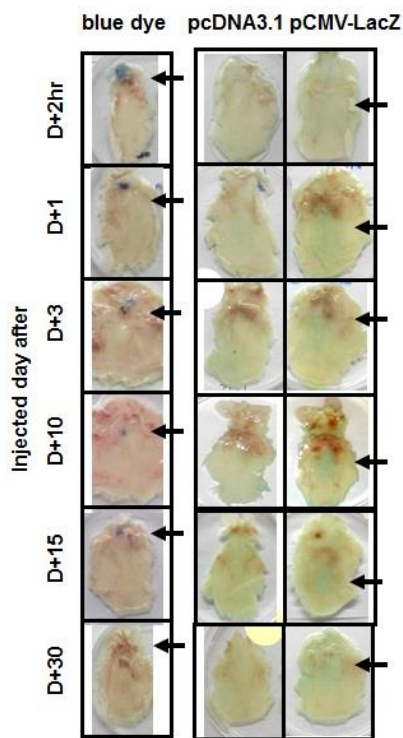
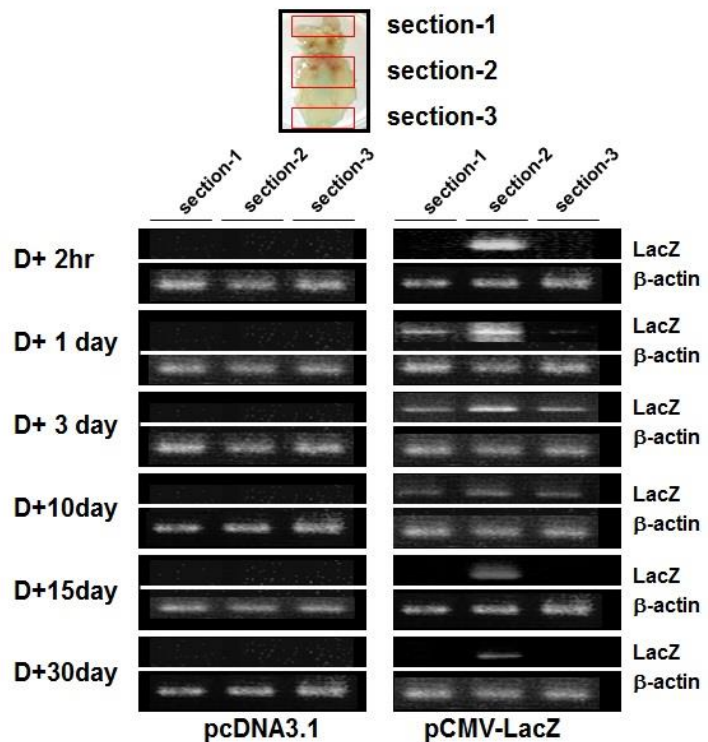
480 measured using a gamma counter 48 h after transfection of pcDNA-hNIS into the cells. Three

481 independent experiments were performed with one representative example shown.

482

483

484

(A) protein expression**(B) existence of LacZ-DNA**

486

487 **Figure 2. In vivo X-gal staining and detection of *lacZ* DNA uptake by cells.** Mice received488 i.d. injection of 100 μ g pCMV-LacZ DNA and in vivo plasmid DNA trafficking was monitored.

489 (A) LacZ protein was detected by X-gal staining at the indicated times. (B) RT-PCR was used

490 to monitor the movement of *lacZ* DNA taken up by cells. The whole dorsal skin was divided

491 into three sections (1, 2, and 3: upper, middle [including injection site], and lower sections,

492 respectively).

493

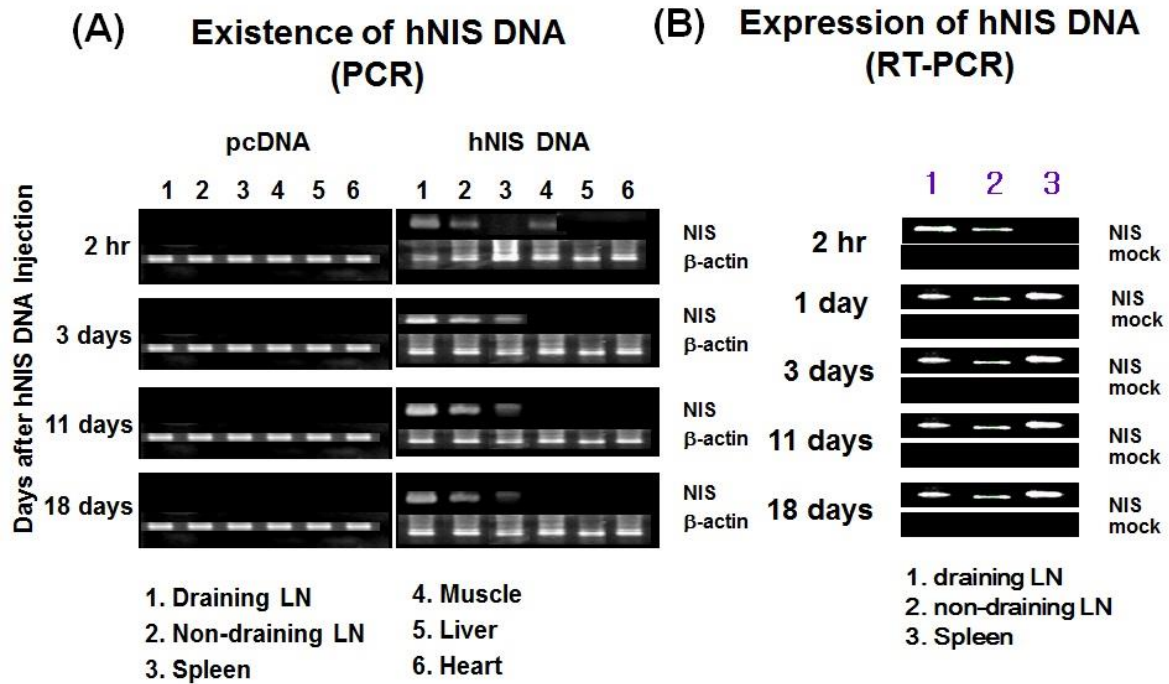
494

495

496

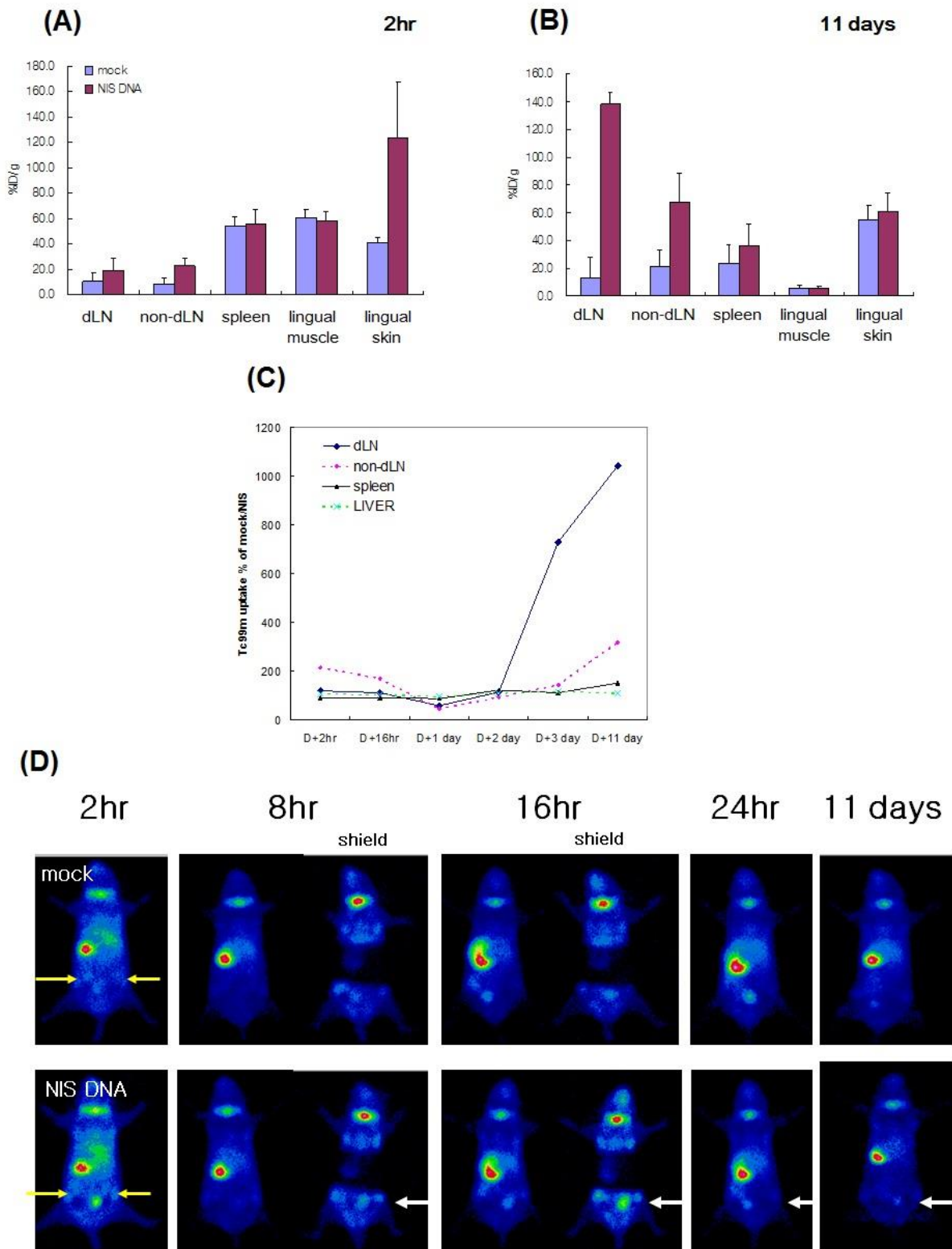
497

498



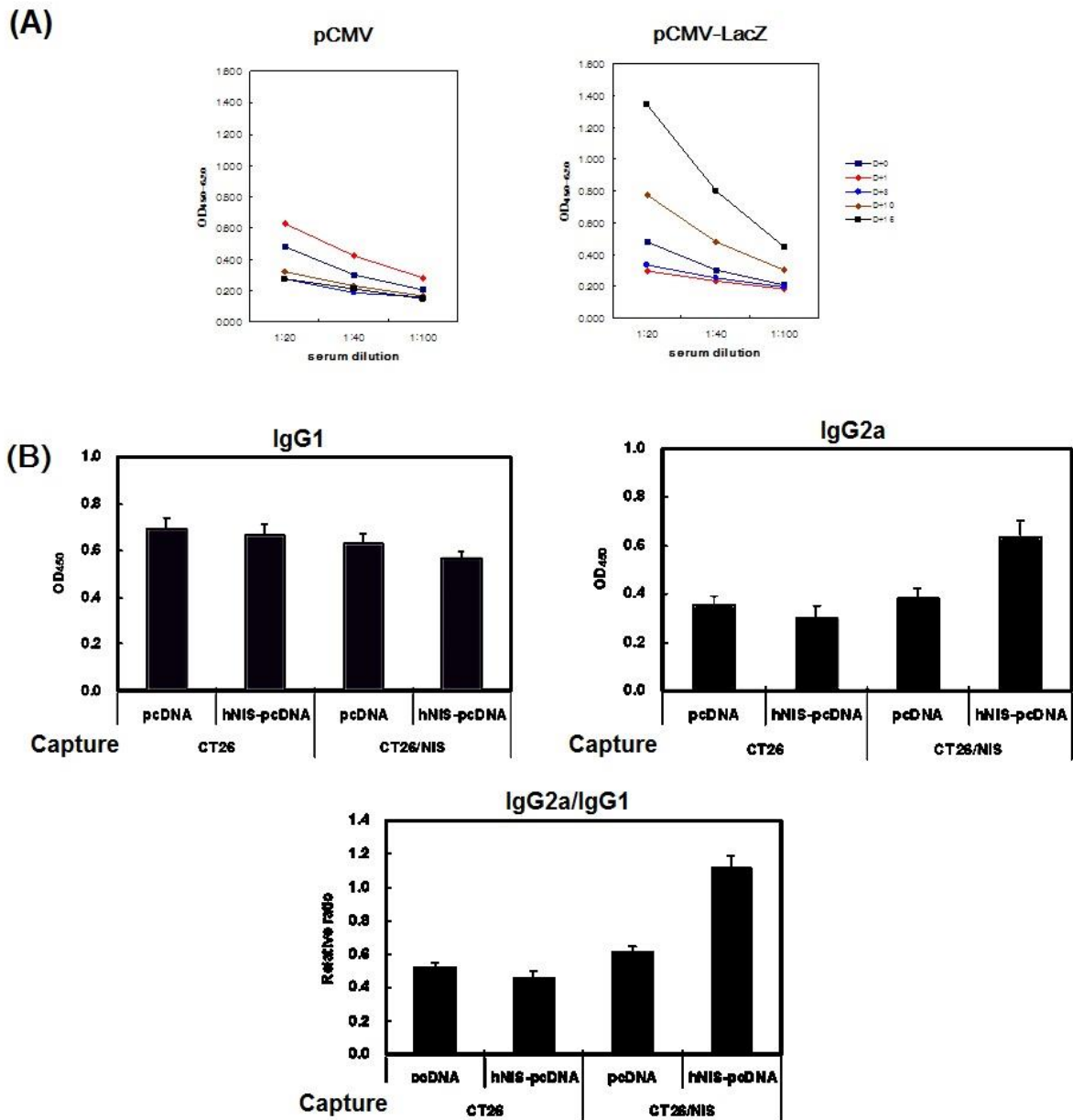
499

500 **Figure 3. In vivo expression of *hNIS* DNA following injection.** (A) The movement of *hNIS*-
 501 expressing cells and transgene expression was monitored by RT-PCR analysis dLNs, non-dLNs,
 502 spleen, lingual muscle, liver, and heart following *hNIS* DNA injection at the indicated time. (B)
 503 RT-PCR in immune organs (dLNs, non-dLNs, and spleen) at various time points.



504

505 **Figure 4. Trafficking of plasmid DNA.** γ -Rays were detected using a gamma counter (A) 2 h,
 506 (B) 11 days, and (C) 0–11 days after hNIS DNA injection into mice. Immune organs (LNs and
 507 spleen), lingual muscle, and lingual skin near the injection site were monitored. (D) Whole-
 508 body imaging of immunized mice with nuclear scintigraphy.



509

510 **Figure 5. Humoral immunity after DNA vaccination.** (A) Serum antibody specific for β -gal.

511 Serum samples were diluted 1/20, 1/40, and 1/100. (B) IgG1 and IgG2a titers against NIS in

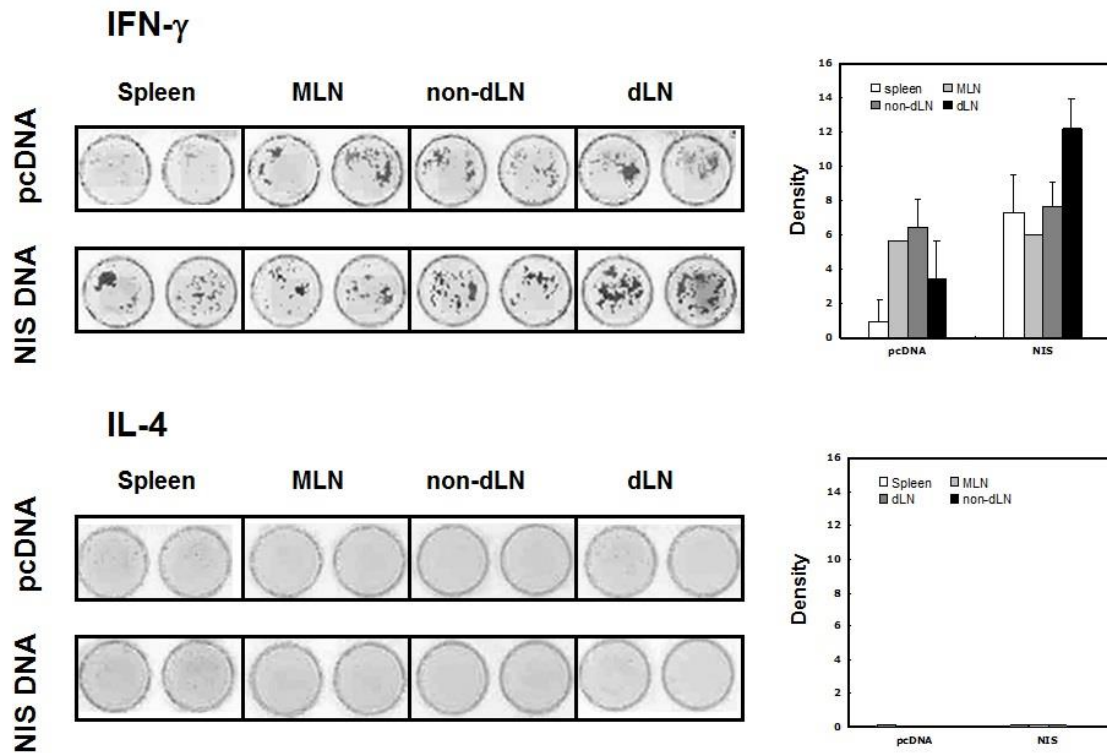
512 the sera of *hNIS* DNA-immunized mice. At 10 days after final injection of *hNIS* DNA (6 weeks

513 after the first immunization), serum samples were collected and anti-NIS IgG1 and IgG2a titers

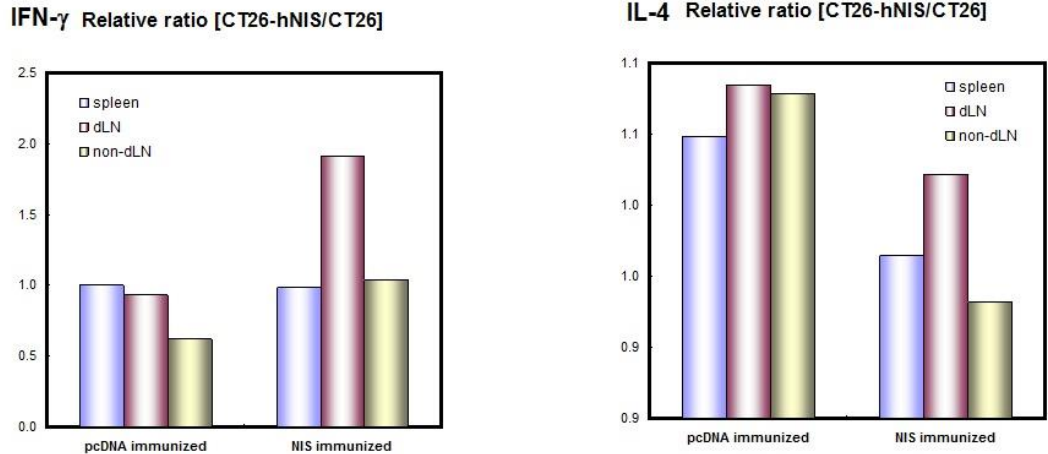
514 were determined by ELISA. IgG1 or IgG2a levels in the serum of pCDNA-NIS- or pCDNA-

515 injected mice were compared to those in the sera (1/100 dilution).

(A) ELISPOT

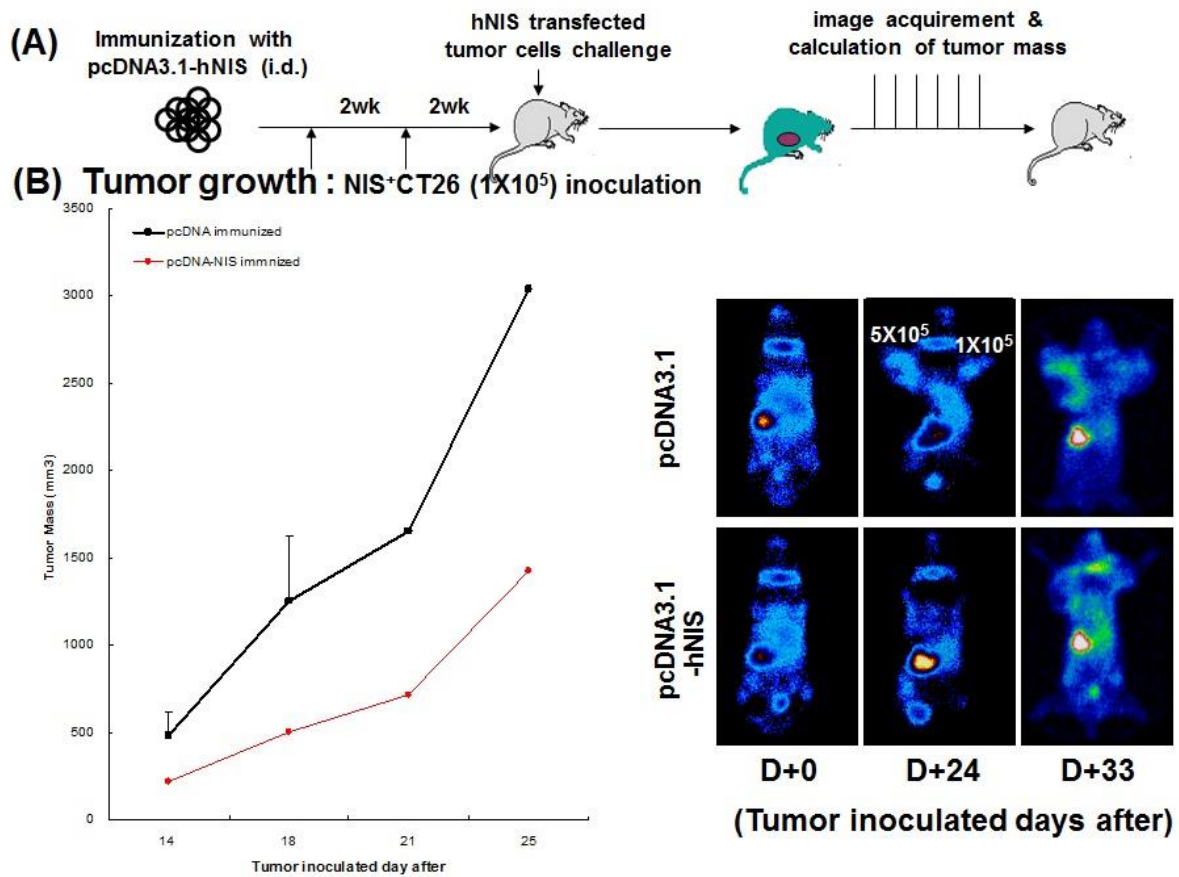


(B) ELISA



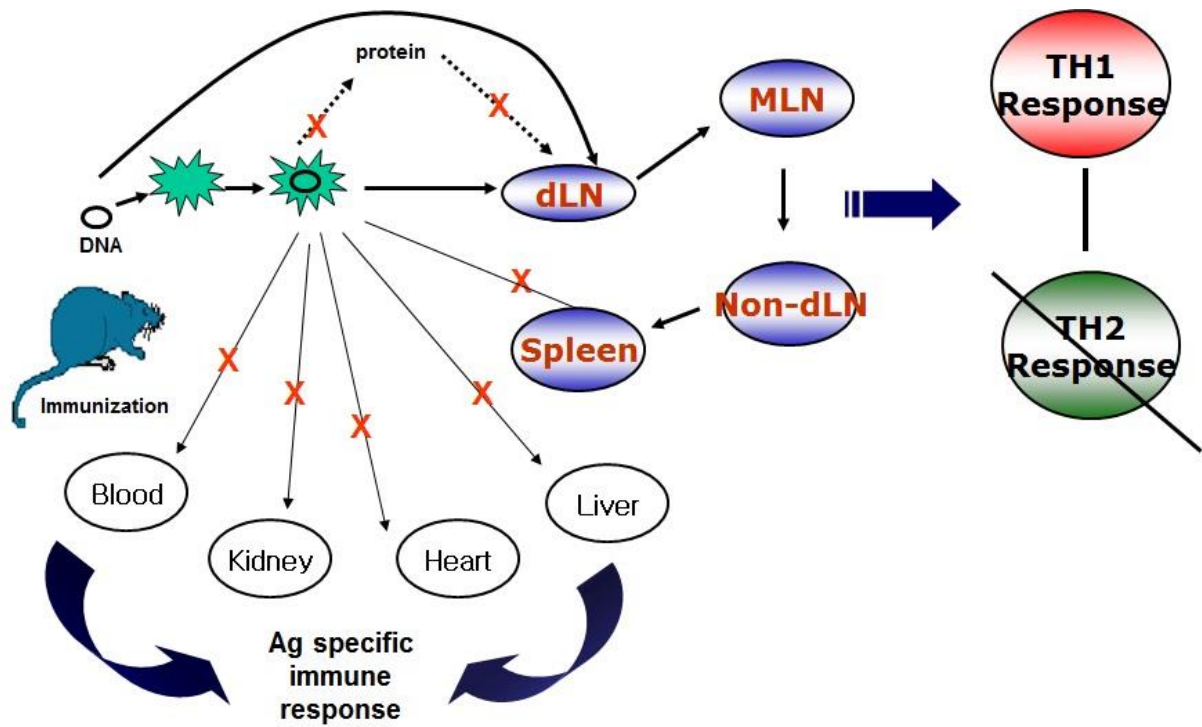
516

517 **Figure 6. Cellular immunity following DNA vaccination.** (A) ELISpot detection of IFN- γ -
518 or IL-4-expressing cells. LNs were collected from *hNIS* DNA-immunized mice and immune
519 cells were isolated with a needle. Cells were cultured for 48 h and IFN- γ or IL-4 levels in the
520 supernatant were determined. (B) Cytokine ELISA detection of IFN- γ or IL-4 in the
521 supernatant of immune cell cultures; the cells were re-activated with irradiated CT26-NIS cells
522 for 48 h before IFN- γ or IL-4 levels in the supernatant were detected.



523

524 **Figure 7. Decrease in tumor growth rate by *hNIS* DNA immunization.** (A) Tumor
 525 inoculation scheme. (B) Tumor retardation after NIS immunization. Left panel shows tumor
 526 growth following inoculation of the fore leg with 1×10^5 CT26/NIS cells; right panel shows
 527 the tumor mass after ^{99m}Tc injection into NIS-immunized mice. Left: 5×10^5 ; right: 1×10^5 .



528

529 **Figure 8. Summary of DNA immunization.** Schematic representation of the mechanism by

530 which DNA immunization results in DNA uptake and cell migration.